Computers and Electronics in Agriculture 196 (2022) 106861

Contents lists available at ScienceDirect

Computers and Electronics in Agriculture

journal homepage: www.elsevier.com/locate/compag

The *spectralrao-monitoring* Python package: A RAO's Q diversity index-based application for land-cover/land-use change detection in multifunctional agricultural areas

Andrea Tassi [a], Andrea Massetti [a], Artur Gil [b,c,*]

[a] Faculty of Sciences and Technology, University of the Azores, 9500-321 Ponta Delgada, Portugal
[b] IVAR -Research Institute for Volcanology and Risks Assessment, University of the Azores, 9500-321 Ponta Delgada, Portugal
[c] cE3c – Centre for Ecology, Evolution, and Environmental Changes & ABG - Azorean Biodiversity Group, Faculty of Sciences and Technology, University of the Azores, 9500-321 Ponta Delgada, Portugal

ARTICLE INFO

Keywords:
Agricultural monitoring
Land-use change
Land-cover change
Agri-environmental indicators
Landsat 8

ABSTRACT

Monitoring multifunctional agricultural areas is paramount to ensure their cost-effective management. The remote sensing-based detection of land-cover/land-use (LCLU) changes and analysis of vegetation dynamics constitute a relevant indicator to support robust monitoring schemes, allowing the control of agri-environmental conditions and enforcing related measures and policies. The Rao's Q diversity index (RaoQ) is frequently used to measure functional diversity in ecology, thanks to the textural analysis of the environment. This paper aims to develop and provide an open-source Python application whose workflow may constitute a RaoQ-based LCLU change monitoring tool for multifunctional agricultural areas. Here, a use case is presented for detecting and mapping LCLU changes leveraging the free and open access Landsat 8 (L8) satellite data. The workflow is organized in four main stages: (1) data processing; (2) Normalized Difference Vegetation Index (NDVI) calculation; (3) RaoQ calculation; and (4) detection and mapping of LCLU changes through thresholding of RaoQ. Three methodological approaches were developed (RaoC – "classic" RaoQ; RaoMD – "multidimensional" RaoQ, and "classic + multidimensional" RaoQ) with overall accuracies ranging from 0.88 to 0.92. An example of an agri-environmental monitoring decision-support framework based on spectralrao-monitoring is presented. The application is easily reproducible, and the code is fully available and utilizable with other sensors at different resolutions to support monitoring other types of agricultural areas.

1. Introduction

The multifunctionality could be the driver of the future of sustainable rural development (Huylenbroeck and Durand, 2003). In fact, it is considered a promising framework of analysis of transformations in agriculture (Cairol et al., 2009; Wilson, 2009). This concept is related to the social, environmental, and ethical services crucial for the society that can be provided by the agricultural and food production sectors (Casini et al., 2012). A multifunctional farming system creates value significantly beyond the mere collection and commercialization of the harvested products (Slámová and Belčáková, 2019). It represents one of the essential aspects of sustainable rural development (Gullino et al., 2018). In these terms, agricultural production presents the opportunity to create various interconnected benefits beyond the main harvested products. It may provide environmental services such as the control of soil health (Williams et al., 2020) and biodiversity (Oliver et al., 2015). Evaluating the effects of different farming systems worldwide is helpful to gauge sustainable agriculture's benefits (Sachs et al., 2010). For this purpose, the European Commission (EC) proposed a set of 28 Agri-Environmental Indicators (AEI) based on the Driver-Pressure-State-Impact-Response approach in the Commission Communication COM final 0508/2006 (European Commission, 2006). Although most of these AEI are based on land-cover/land-use (LCLU), the land-use change (AEI #9) is a relevant AEI for monitoring and assessing socioeconomic and environmental impacts in agricultural areas, particularly in High Nature Value (HNV) farmlands (Gil et al., 2018) because it ties together biodiversity to the continuation of farming on certain types of land and the maintenance of specific farming systems. Land-use change mapping

* Corresponding author.
E-mail address: artur.jf.gil@uac.pt (A. Gil).

https://doi.org/10.1016/j.compag.2022.106861
Received 9 September 2021; Received in revised form 5 March 2022; Accepted 7 March 2022
Available online 24 March 2022
0168-1699/

and monitoring represent significant challenges (Lomba et al., 2014). Identifying the LCLU changes is highly relevant for agroecosystem monitoring, planning, and management. Public institutions use LCLU to help develop new policies, assess the implementation of past and current policies (Johnson et al., 2002), design effective subsidies, and support the decision-making process in urban planning and development (Thunig et al., 2011). Other agencies, such as NGOs and private enterprises, use LCLU for a range of applications, including monitoring of the crop yields and productivity (Lobell et al., 2015), analysis of forest degradation, and illegal logging activities (Hansen et al., 2013), handling of critical animal habitats, biological hotspots and restoration and rehabilitation under disaster management (Balamurugan and Aravind, 2015). The study of LCLUC can help shed light on the current global issues, like melting of ice, modified rainfall patterns, abnormal temperatures, monitoring coastal change (Tassi and Gil, 2020), urban sprawl (Aboelnour and Engel, 2018), conflicts, and food security (Abdulkareem et al., 2018) agricultural field (Ramankutty and Foley, 1999), water bodies (Costa et al., 2003) and about woodlands and forests (Hansen et al., 2014). Techniques based on multi-temporal multi-spectral satellite data have demonstrated the potential to detect, identify, map, and monitor ecosystem changes, irrespective of their causal agents. However, there are several challenges facing ecosystem change monitoring from space, namely: (i) to detect the arising new types of land use, in addition to conversions from already present land uses; (ii) to monitor rapid and abrupt changes, as well as the progressive and incremental changes; (iii) to separate inter-annual variability from secular trends, given the reduced length of the available time series; (iv) to understand and correctly address the variations deriving from the spatial scale dependence of statistical estimates of change at different spatial resolutions; and (v) to match the temporal sampling rates of observations of processes to the intrinsic scales of these processes (Coppin et al., 2004).

The use of the spectral indices allows highlighting the changes. The Normalized Difference Vegetation Index (NDVI) (Rouse et al., 1974) is widely used because it directly expresses a measure of vegetation health. It is common to detect the changes in the Earth's surface (Lunetta et al., 2006; Woodcock et al., 2010). The combination of its normalized difference formulation and the use of the highest absorption and reflectance regions of chlorophyll make it robust over a wide range of conditions (Tassi et al., 2021). In a review, Rocchini *et al.* (Rocchini et al., 2010) summarized several approaches to measure ecosystem diversity from remotely sensed images. Those approaches are mainly based on the spatial variability of the reflectance value recorded by multispectral sensors. In this context, the Spectral Variation Hypothesis (SVH) is defined as the higher the spectral variation exhibited by such satellite sensor acquisitions, the higher the environmental heterogeneity and thus the species diversity of that area. High-resolution multispectral satellite data can contribute to the biodiversity assessment of complex ecosystems (Rocchini et al., 2004; Palmer et al., 2002). The pixel-to-pixel variability of the spectral response in a remotely sensed image is driven by multiple factors in variable proportion depending on the observation scale (Torresani et al., 2021). The emergence of SVH has gained widespread attention in the remote sensing community, especially as a method for deriving biodiversity information from remotely sensed data (Madonsela et al., 2021). Several studies have tested SVH in different ecosystems, using various spectral heterogeneity metrics, and observed varying levels of relationships between spectral heterogeneity and species diversity (Schmidtlein & Fassnacht, 2017). Nevertheless, there is some criticism about the SVH hypothesis. Schmidtlein & Fassnacht (2017) observed that high spectral heterogeneity does not always correspond to high species richness and vice versa, being SVH ecosystem dependent. Rocchini et al. (2017) have demonstrated the potential advantages of applying the SVH to remote sensing data through the determination of RaoQ, to calculate diversity in digital imagery.

The RaoQ was initially developed by Rao (1982) and introduced by Botta-Dukát (2005) to measure functional diversity in ecology. Given a subset MxM pixels of an NxN image, where M is an odd number, the RaoQ is proportional to the sum of all the pixel values pairwise distances, weighted by the relative abundance of each pair of pixels in the analyzed image. In other words, RaoQ is the expected difference in reflectance values between two pixels drawn randomly with replacement from the considered evaluated pixels set. Most commonly, the RaoQ is calculated from pixel values from combinations of the satellite spectral bands (Zhang et al., 2017), such as the NDVI index is used as input (Khare et al., 2021). Furthermore, the potential to explore multiple combinations of spectral bands is derived from the utilization of the Near-Infrared (NIR) and from the information of the Shortwave Infrared (SWIR) to calculate the vegetation indices most sensitive to phenological variations (Chaves et al., 2020).

An additional point is computational; in fact, the remote sensing data processing procedure has been mainly based on traditional workstations, benefitting from limited computational resources and implying relevant limitations on managing vast amounts of data, storage, and analysis. Although Sentinel-2 data has a higher spatial resolution than Landsat-8 data, we decided to use the latter because of its faster computational processing. Furthermore, the main advantage of Landsat-8 data is providing a nearly 60-year long and uninterrupted historical archive that allows doing these same analyses using much larger temporal ranges. Congedo (2019) provided cost-effective GIS-based tools for the download, preprocessing, and post-processing of images, but the performance in terms of speed is still related to the workstation's characteristics. The use of cloud-based platforms (i.e., Google Earth Engine - GEE) allows their users to instantly access and analyze geospatial data through web interfaces (Gorelick et al., 2017) and obtain, for example, LCLU classification maps without the use of local resources (Tassi and Vizzari, 2020). This paper aims to develop and provide an open-source Python application whose workflow may constitute a RaoQ-based LCLU change monitoring tool for multifunctional agricultural areas. This application will also support the semi-automatic and cost-effective monitoring of the agri-environmental indicator (AEI) #9, "land-use change", proposed by the European Commission in the Commission Communication COM final 0508/2006 (European Commission, 2022). To achieve this goal, two main research questions are addressed in this methodological proposal: (1) Are RaoQ-based approaches effective for detecting and mapping LCLU changes in LCLU-diverse areas as the multifunctional agricultural sites?; and (2) Is the "classic" and computational low-cost NDVI-based RaoQ calculation enough to effectively detecting and mapping LCLU changes in multifunctional agricultural sites, or do we need more complex approaches (e.g., multidimensional and classic + multidimensional) for achieving more reliable results?

2. The spectralrao-monitoring Python package

The open-source repository called *spectralrao-monitoring* is available on GitHub at https://github.com/AndreaTassi23/spectralrao-monitoring. The user can find the methods implemented on Python3 to replicate the result of the work.

A function called *spectralrao* was implemented, being the code a free port of the original R code published by Rocchini et al. (2017). This R code has also been implemented in the R rasterdiv package, *rasterdiv-an* (Rocchini et al., 2021). This function is based on the following Python packages: *NumPy*, *pandas*, *math*, *rasterio*, *combination*, and *matplotlib*. The function receives one or more rasters as input and converts them to a NumPy 2d array. *Spectralrao* function performs all the steps needed to retrieve the RaoQ index and saves the output as a GeoTIFF raster in the desired path. The function supports two different modes of use: (i) "*classic*" calculates RaoQ on a single raster layer (or band); and (ii) *multidimensional*, making use of several bands defined by the user. In both cases, a window size parameter given by the user is required to define an odd-sized square rolling window to preserve the integrity of the information - the movement of the window on the whole image allowing to iterate the procedures to define RaoQ. A larger window size allows covering a broader area in a single pass of the moving window. Another argument is called *na.tolerance*, and it determines the algorithm's behavior when encountering Not a Number (NaN) values in the input image. This parameter represents the minimum number of finite values accepted, enabling the calculation of the RaoQ in any given rolling window. In the *multi-dimensional* mode, the distance matrix is used to compare and assess the similarity of the input bands for the definition of RaoQ. According to the specific user needs, the distance matrix used can be controlled by specifying the optional parameter *distance_m*. Possible choices are Euclidean or Manhattan distance to produce multivariate measures of dissimilarity (Podani, 2000).

The identification of the change that occurred in the time is based on a threshold computed using the secant method (Vázquez-Jiménez et al., 2018) that allows representing in a histogram the distribution of the pixels and the automatic position of the threshold. This is defined using two methods available in the Python package: *calculateDistance* used to calculate the distance between two points. It is mandatory to compute the *threshold_method* to determine the interest value to define the limit to certificate a change. This last method requires as input the NumPy type difference between the RaoQ for two periods of interest, being the result a binary map (Change-NoChange).

The Python3 methods available allowed to compare two different binary maps with the same shape and a NumPy type as input. The output of the b*inary_change* is a single binary map where the change is confirmed only when it occurred in the same pixel of two different inputs. The priority assessment framework's example developed within this case study (see 4.2), synthesized in Table 2, supports more robust and cost-effective LCLU change-related controlling schemes in CAP-subsidized multifunctional agricultural areas. The method, *priority_classification*, requires the input of the two binary maps extracted using RaoQ and NDVI information and allows defining the priority of the change for each pixel of the area of interest.

3. Material and methods

3.1. Study area

The study area selected to develop, test, and validate the work is a multifunctional agricultural area of 11,871 ha called "Charneca do Infantado", located in Portugal's Ribatejo region (Fig. 1). This territory is part of the estate "Companhia das Lezírias S.A", which is the largest Portuguese multifunctional farmstead located on the left margin of the Tagus River (38° 52′ 48″ N, 08° 51′ 08″ W; Central Portugal). A multifunctional landscape mosaic characterizes the area of interest with high abundance and diversity of agricultural lands (e.g., rice fields, irrigated forages, pastures, cork oak woodlands, and pine forests).

3.2. Methodological workflow

The methodological workflow of this application is constituted by four main steps (Fig. 2). First, L8 remote sensing data were downloaded and corrected. The NDVI processing phase allowed the production of NDVI maps to support the production of RaoQ-based maps. RaoQ and a thresholding method were combined to produce the binary map to define the changes, minimizing "false changes". In this methodological approach, we assumed that "false changes" only refer to detected changes in any of the two initial RaoQ-based approaches, RaoC and RaoMD, that were not confirmed in the other RaoQ-based approach (e.g., a pixel classified as "change" in the RaoC approach and classified as "no-change" in the RaoMD approach). The maps allowed to identify and quantify each class's changes from 2015 to 2018 in the spring growing season (SGS).

3.2.1. Prospection, preprocessing, and organization of L8 data

The L8 multispectral bands covering the case-study area were obtained at the Terrain Precision Correction processing level (L1TP). In particular, bands 4 (B4, Red: 0.630–0.680 μm), 5 (B5, NIR: 0.845–0.885 μm) and 6 (B6, SWIR-1: 1.560–1.660 μm) were acquired for four

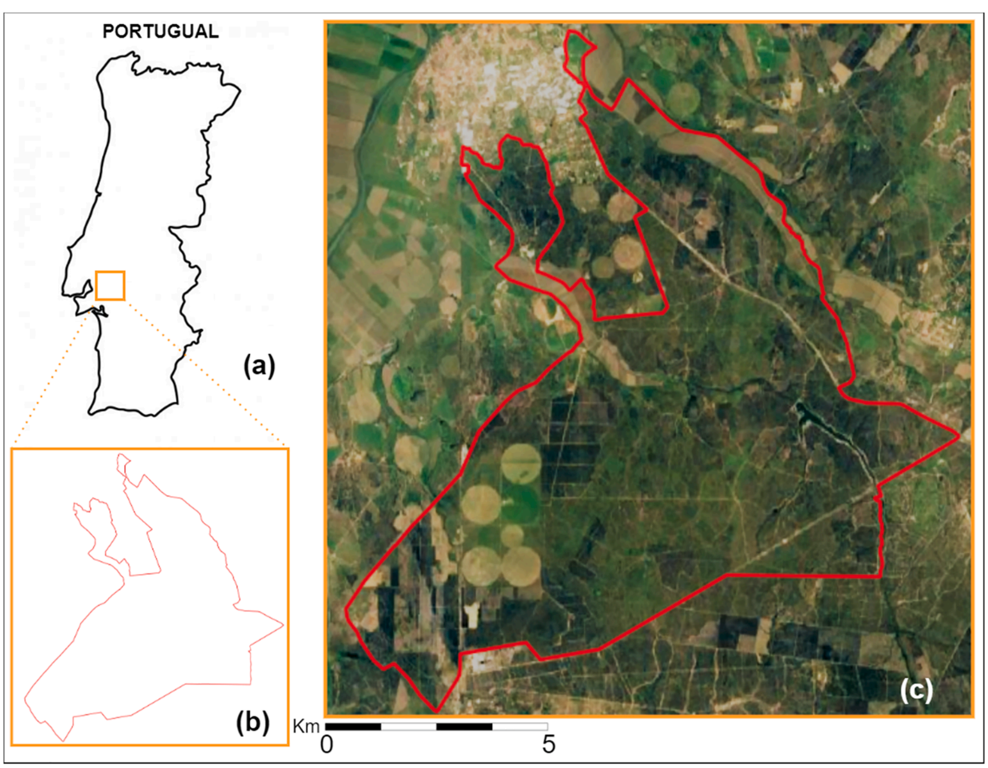

Fig. 1. Location of the multifunctional agricultural study area in Ribatejo, Portugal (a). An overview of "Charneca do Infantado" (b) and the RGB image (c) based on Landsat-8 bands.

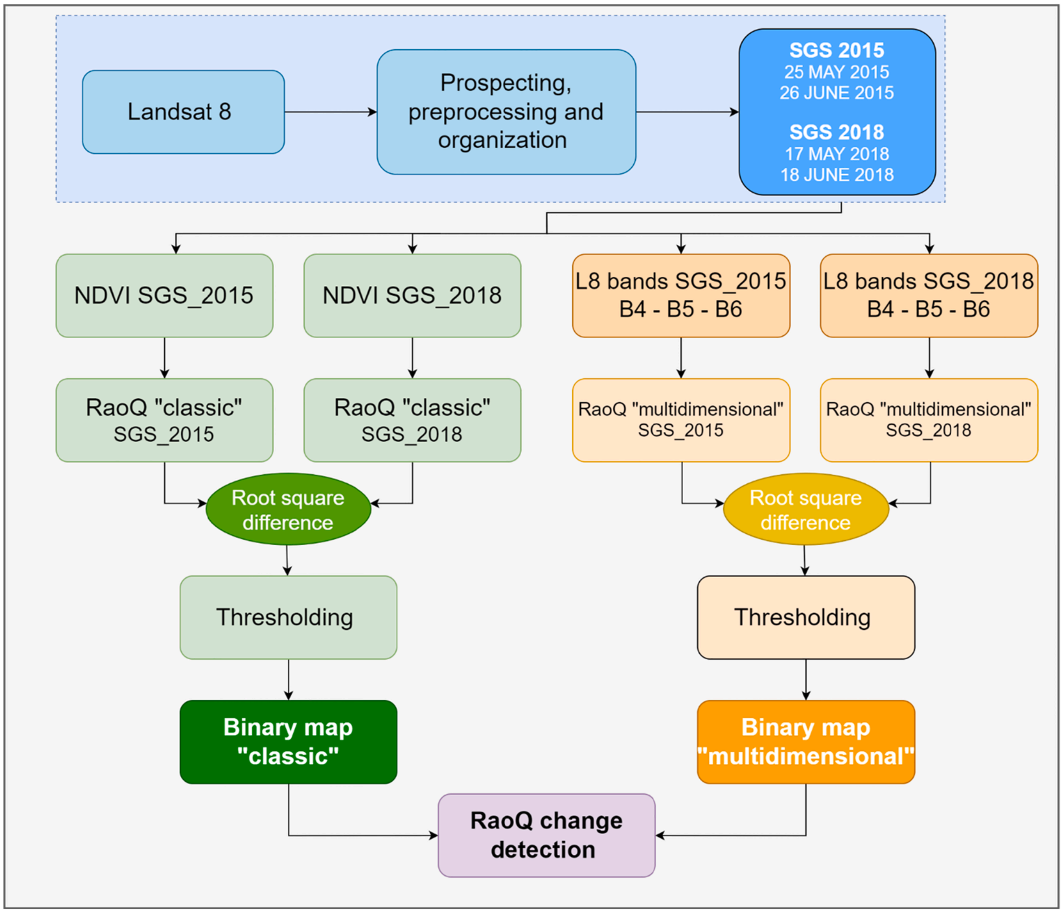

Fig. 2. Methodological flowchart.

different dates, respectively 25 May 2015, 26 June 2015, 17 May 2018, and 18 June 2018. The imagery was atmospherically corrected using the Dark Object Subtraction (DOS) method (Chavez, 1996). Next, the average value was computed for each pixel between two periods during the spring growing season (SGS): May/June 2015 (producing the averaged data set SGS_2015) and May/June 2018 (producing the averaged data set SGS_2018). This step mitigated the influence of small changes between bands from the same season and year, thus reducing the relative differences from phenological and meteorological conditions, and was performed separately for the two different years, 2015 and 2018.

3.2.2. NDVI processing

The average data generated in the previous step was used to compute the NDVI. An NDVI map was produced for both SGS_2015 and SGS_2018 data sets. To illustrate, at the end of this article, a potential example of an agri-environmental policy-support application, a 2015–2018 NDVI changes map (ΔNDVI_2015-2018), was created as the square root of the squared difference between the two NDVI maps (Shao et al., 2016) (Eq. (1)):

$$\Delta \mathrm{NDVI}_{2015-2018} = \sqrt{(NDVI_{2018} - NDVI_{2015})^2} \quad (1)$$

The resulting map was divided in three ranges of NDVI change values: (i) < 0.2: No/Low Change; (ii) 0.2 to 0.4: Medium Change; and (iii) > 0.4: High Change.

3.2.3. RaoQ processing

RaoQ maps were calculated for SGS_2015 and SGS_2018, respectively, using two approaches: (i) the one-band or “classic” approach (RaoC) directly derived from each average NDVI map previously defined, following (Rocchini et al. (2017)); and (ii) the multi-band or“ multi-dimensional” approach (RaoMD) using for each period a combination of the average values of three vegetation-relevant L8 spectral bands, namely B4 (Red), B5 (NIR) and B6 (SWIR-1). This innovative band combination improved spectral information to calculate the vegetation indices most sensitive to phenological variations (Chaves et al., 2020). The same input parameters are used for both approaches: the window’s dimension defined is 3, and the na.tolerance is set 0. Afterward, two 2015–2018 RaoQ maps were produced by applying the root square difference to the RaoC (Eq. (2)) and RaoMD (Eq. (3)) approaches, respectively:

$$RaoC_{2015-2018} = \sqrt{(RaoC_{2018} - RaoC_{2015})^2} \quad (2)$$

$$RaoMD_{2015-2018} = \sqrt{(RaoMD_{2018} - RaoMD_{2015})^2} \quad (3)$$

3.2.4. Threshold-based change detection

The difference between each pair of RaoQ maps (RaoC_2015-2018 or RaoMD_2015-2018) is defined by the pixel values corresponding to the intensity of the change estimated. For each methodological approach (“classic” or “multi-dimensional”), a final binary map using two classes, “Change” and “No Change”, was generated based on a threshold value. The secant method determined the optimal threshold (Ramos-Bernal et al., 2018). This threshold is defined by the value corresponding to the point in the histogram distribution of all pixel values, where the maximum perpendicular line intersects the secant line between the highest and lowest points of the histogram (Fig. 3). The classic approach produced a threshold of 0.031, while the value for the multi-dimensional approach is 0.047. Afterward, both “Change/No Change” binary maps

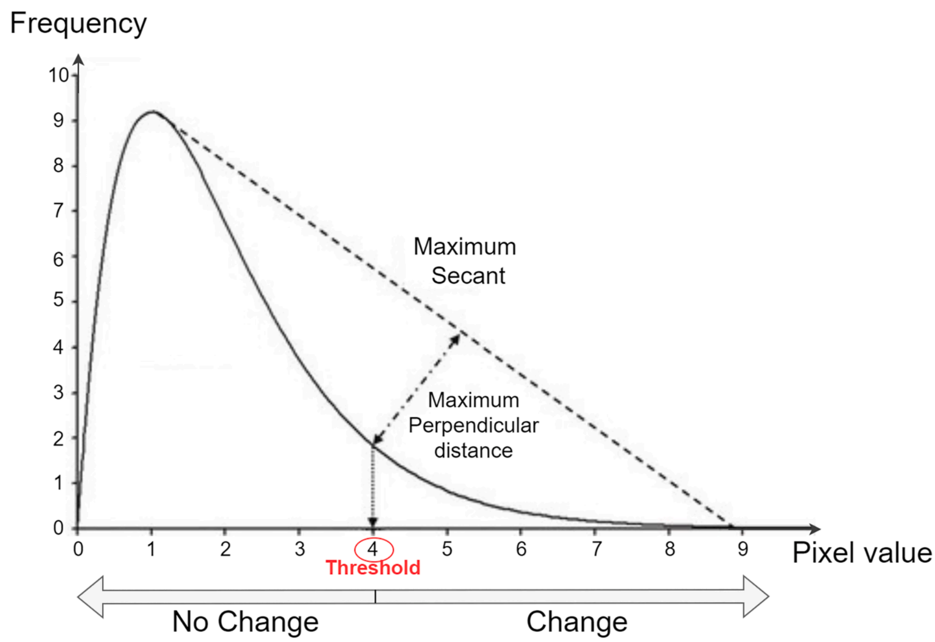

Fig. 3. The secant method used to detect the threshold according to Ramos-Bernal et al. (2018).

derived respectively from RaoC_2015-2018, and RaoMD_2015-2018 were overlaid to produce a final and unified RaoQ_2015-2018 "Change/No Change" binary map assuming as "changed areas" only pixels with this same classification in both approaches' outputs. This idea reduced the "false positive" changes, as referred to previously. The change is confirmed only when it occurs in both binary maps.

3.2.5. Overall accuracy assessment

To assess the accuracy of each RaoQ-based methodological approach's binary map results (RaoC, RaoMD, and "classic +

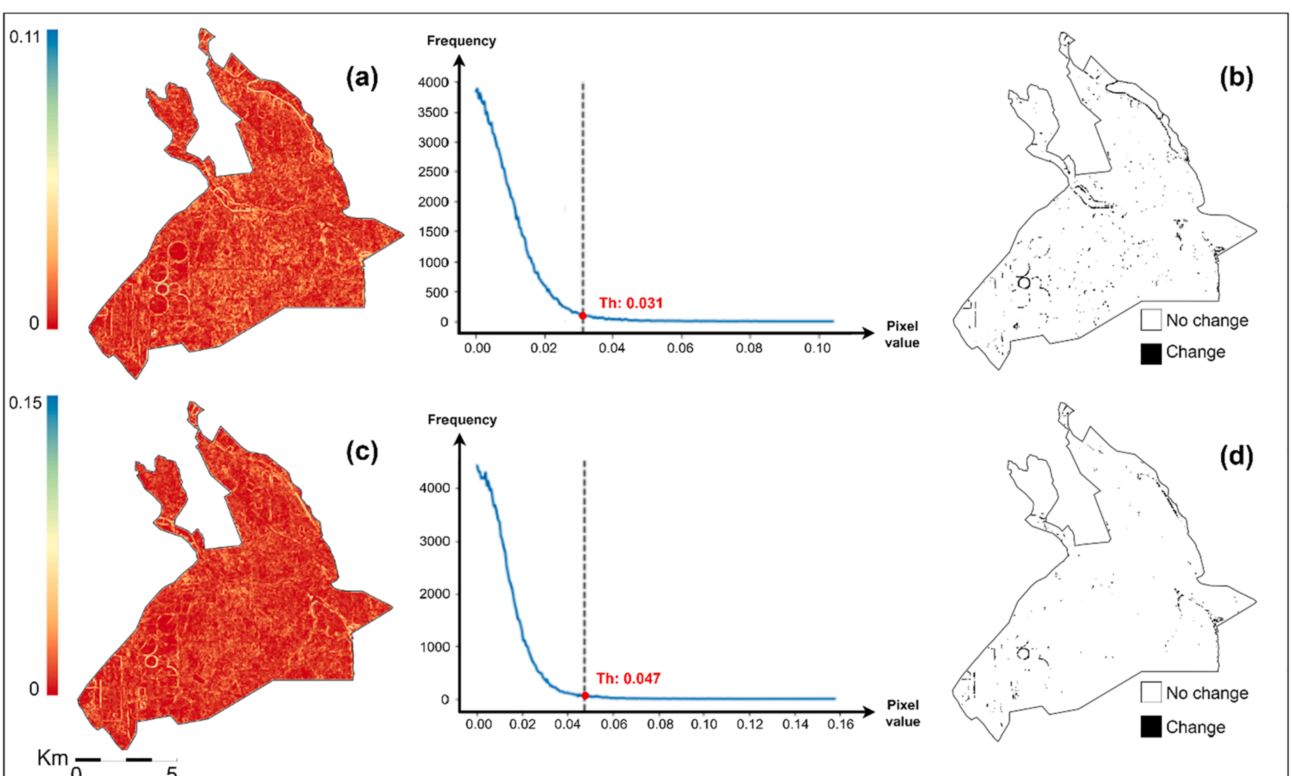

Fig. 4. In the horizontal sequence at the top, RaoQ-based change detection through thresholding using the RaoC approach. Figure (a) shows the RaoQ root square difference relative to the period of interest SGS_2015 - SGS_2018. The threshold obtained is Th = 0.031, and it is used to define the binary map (b), highlighting the changes obtained with the "classic" method. In the horizontal sequence at the bottom, the RaoMD approach. Figure (c) shows the RaoQ root square difference relative to SGS_2015 - SGS_2018. The threshold value for this method is Th = 0.047 which is used to define the binary map that highlights the changes that occurred in the "multidimensional approach" (d).

multidimensional"), the respective overall accuracy (Lillesand & Kiefer, 2000) was computed by producing and evaluating for each binary map a random 100-points dataset (shapefile format) with 50 change and 50 no-change points. These three validation datasets were assessed through a GIS-based comparative photo-interpretation of two high spatial resolution Rapideye satellite images of the case-study area, acquired respectively at 18 June 2015 and 16 June 2018. The identification of change/no change in LCLU among both dates (2015–2018) was the photo interpretation criteria used for classifying the change/no change classification obtained with each RaoQ approach as correct/incorrect.

4. Results

4.1. The RaoQ-based monitoring framework for LCLU change detection in multifunctional agricultural areas

The *spectralrao-monitoring* workflow led to the development and validation of an innovative, free, and open-source python application able to constitute a RaoQ-based LCLU change monitoring tool in multifunctional agricultural areas. The calculation of RaoQ was used in both the "classic" (RaoC) and "multi-dimensional" (RaoMD) approaches to defining the root square difference relative to the period of interest. According to the secant method, the latter allowed to determine the automatic threshold and the subsequent binary maps ("no-change" versus "change") derived as shown in Fig. 4.

The information extracted from the RaoQ-based change detection method using the "classic" and "multi-dimensional" approaches was combined to get a unique binary map representing the identification of LCLU changes in the study area ("classic + multidimensional").

Table 1 shows the overall accuracy results obtained for each one of the RaoQ-based methodological approaches. The approach showing best results ("classic + multidimensional") was the one selected to illustrate a potential example of an agri-environmental policy-support application (4.2).

4.2. Example of a policy-support application: Monitoring and controlling vegetation and LCLU changes in a CAP-subsidized multifunctional agricultural area - Charneca do Infantado (Portugal)

As the introduction mentioned, LCLU change (AEI #9) is one of the 28 agri-environmental indicators proposed by the European Commission, as identifying the LCLU changes is highly relevant for agro-ecosystem monitoring, planning, and management. Furthermore, the development of robust, reliable, (semi-)automatized and cost-effective LCLU changes monitoring tools might allow a better assessment of socioeconomic and environmental impacts in agricultural areas, providing, therefore, relevant information to support public institutions (e.g., the European Commission and the national authorities in agriculture and rural development) in improving public policies development and assessment (e.g., CAP - EU's Common Agricultural Policy: design of agri-environmental schemes and public subsidies; monitoring and assessment of CAP measures; etc.). To illustrate the potential of our tool for monitoring LCLU changes in multifunctional agricultural areas as "Charneca do Infantado" (Portugal), we present below an example of a simple decision-support framework aiming at more robust, reliable, and cost-effective management by public entities – namely the national/regional authorities on CAP-subsidizing monitoring. Its use might avoid unnecessary and expensive on-site LCLU-related control actions and focus their limited (economic, human, and logistic) resources in the more problematic areas, where relevant LCLU/vegetation changes are effectively detected.

Table 1
Overall accuracy results obtained for each one of the RaoQ methodological approaches.

Method	Overall Accuracy
RaoC	0.91
RaoMD	0.88
"classic + multidimensional"	0.92

Fig. 5 shows the visual comparison between the NDVI-based change detection classification (see 3.2.2) and the RaoQ-based change detection by using the "classic + multidimensional" approach, which showed the higher overall accuracy (0.92) from all three previously tested RaoQ-based approaches.

By overlaying both layers, the different combinations of ΔNDVI_2015-2018 and ΔRaoQ_2015-2018 values (Table 2) can be used by the Portuguese national public authority on CAP-subsidizing and monitoring (IFAP – *Instituto de Financiamento da Agricultura e Pescas*) to assess, rank, and map their priorities in controlling the LCLU/vegetation change-related actions in "Charneca do Infantado". Table 2 displays a hypothetical example of how an entity like IFAP could address their priority assessment and management for on-site control actions: Low Priority Areas (P0, with no changes in RaoQ-based LCLU status and NDVI-based vegetation status); Medium Priority Areas (P1, with no changes in RaoQ-based LCLU status and with relevant changes in NDVI-based vegetation status); and High Priority Areas (P2, with detected changes in RaoQ-based LCLU status and highly-relevant changes in NDVI-based vegetation status).

In the case of this study area, for the experimental period between SGS 2015 and SGS 2018, the quantitative results of using such an approach are reported in Table 3.

The final step of this policy-support operational framework would be overlaying the priority assessment map with a detailed and updated LCLU map (according to the time range considered for analysis), as the one developed by Fernandes et al. (2019) for "*Charneca do Infantado*". The LCLU map generated (Fig. 7) was based on 22 different LCLU/vegetation categories.

According to Fig. 6 and Table 3, most of the study area is classified as showing low priority (P0: not relevant or no changes at all), representing 92.13% of the whole area with approximately 10,936.54 ha. The medium priority area (P1: relevant NDVI-based vegetation status changes) represents 7.36% of the total area, with about 874.14 ha. According to Table 4, P1 areas are mainly associated with Mediterranean cork oak savannas (320.19 ha, 2.70%), irrigated crops (235,19 ha, 1.98%), and rice fields (193.17 ha, 1.64 %). In comparison, a minor contribution is associated with *Eucalyptus* plantations (38.56 ha, 0.33%) and Open areas (22.37 ha, 0.19%) – see Fig. 8.a. Finally, the most critical area showing highly relevant changes (and requiring, therefore, special attention in terms of on-site controlling), classified as P2 (highly relevant NDVI and effective RaoQ-based changes), were identified in about 0.51% (60.60 ha) of "Charneca do Infantado". These LCLU/vegetation changes classified as P2 areas were associated with dynamic agricultural or forest areas with changeable cultures/crops (see Fig. 8.b), which require more intensive and seasonal management measures, namely irrigated crops (18.37 ha, 0.16%), *Eucalyptus* plantations (7.46 ha, 0.063%), floodplain areas (6.59 ha, 0.056%), Mediterranean cork oak savannas (5.09 ha, 0.044%), open areas (4.74 ha, 0.040%), permanent water surfaces (4.35 ha, 0.038%), vineyards (3.89 ha, 0.034%), and rice fields (1.98 ha, 0.018%).

5. Discussion and conclusions

The overall accuracies of 0.91 and 0.88 obtained respectively by the RaoC and the RaoMD approaches showed the effectiveness of using the Rao's Q diversity index to detect and map LCLU changes in diverse and complex landscapes as the multifunctional agricultural areas, positively addressing our Research Question #1. Most detected LCLU changes are associated with dynamic agricultural or forest areas with changeable cultures/crops requiring more intensive and seasonal management measures, namely irrigated crops, production forest plantations, floodplain areas, permanent water surfaces, vineyards, and rice fields.

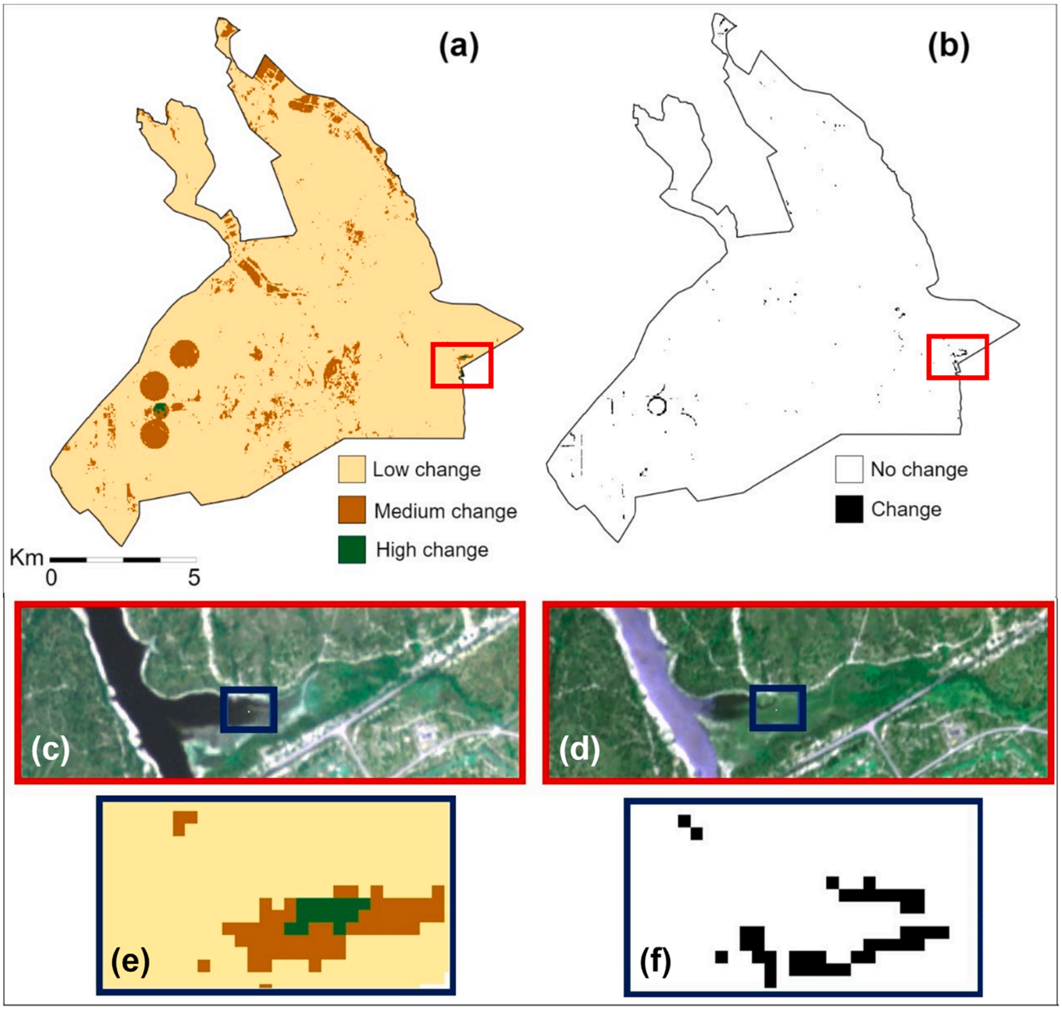

Fig. 5. Comparison between NDVI-based change detection classification (a) and RaoQ-based change detection (b). High-resolution Rapideye's RGB images from June 2015 (c) and June 2018 (d) zooming in the same subarea of interest showing different results for NDVI-based change detection classification (e) and RaoQ-based change detection (f).

Table 2
Hypothetical example of how an entity like IFAP (Portugal) could address their priority assessment and management for LCLU/vegetation-related on-site control actions in multifunctional agricultural areas as "Charneca do Infantado".

	RaoQ NoChange	RaoQ Change
NDVI No/Low change	Low Priority Area (P0)	High Priority Area (P2)
NDVI Medium change	Medium Priority Area (P1)	High Priority Area (P2)
NDVI High change	High Priority Area (P2)	High Priority Area (P2)

Table 3
Quantification and classification of LCLU/vegetation-related on-site controlling actions in "Charneca do Infantado" (after May/June 2018).

Type	Areas (ha)	Areas (%)
P0	10936.54	92.13 %
P1	874.14	7.36 %
P2	60.60	0.51 %

Furthermore, as illustrated in Fig. 5, it constitutes a more reliable approach than using the NDVI changes map (ΔNDVI) solely, as those might not correspond to real LCLU changes. Instead, both ΔNDVI and ΔRaoQ-based information shall be used synergistically to support decision-making, as shown in our "Example of a policy-support application". These results also confirm the indications made by Torresani et al. (2019) and Khare et al. (2021) regarding the effectiveness of using the NDVI-based Rao's Q diversity index (our RaoC approach).

To take advantage of the massive amount of very high/high/medium spatial resolution open and free multispectral data (e.g., Landsat, Sentinel-2, ASTER, SPOT, CBERS), another objective of this research was to test the effectiveness of using a multidimensional approach of the Rao's Q diversity index (our RaoMD approach), using a combination of three selected L8 spectral bands (RED-NIR-SWIR1) meant to take advantage of specific spectral characteristics of vegetation. In this study, the "classic" NDVI-based RaoQ (RaoC) approach performed better than the "multidimensional" (RaoMD) approach (0.91 and 0.88 of overall accuracy, respectively), although the differences obtained between these two approaches were minor. These results positively address our Research Question #2, confirming that using only the NDVI-based RaoQ approach (RaoC) might be sufficient to detect and map LCLU changes in multifunctional agricultural areas effectively. Nevertheless, for future case studies using our *spectralrao-monitoring* script, we recommend users to previously compare and assess the similarity of the selected input multispectral bands by using multivariate measures of dissimilarity (e.g., Transformed Divergence and Jeffries-Matsushita separability assessment). Although both RaoC and RaoMD approaches presented and tested in this study were developed using L8 multispectral data (as explained above), the spatial, spectral, and temporal resolutions of the input bands can be significantly improved by using data from a different

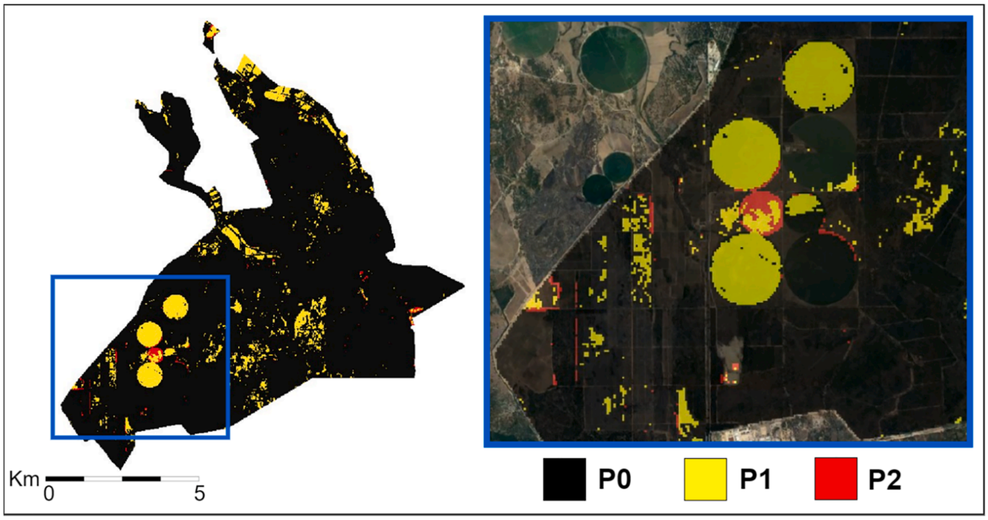

Fig. 6. Hypothetical priority assessment map for IFAP's LCLU/vegetation-related on-site control actions in "Charneca do Infantado," for the period of interest (SGS_2015 - SGS_2018). P0 represents the low priority class, P1 is the medium priority, and P2 is the high priority class.

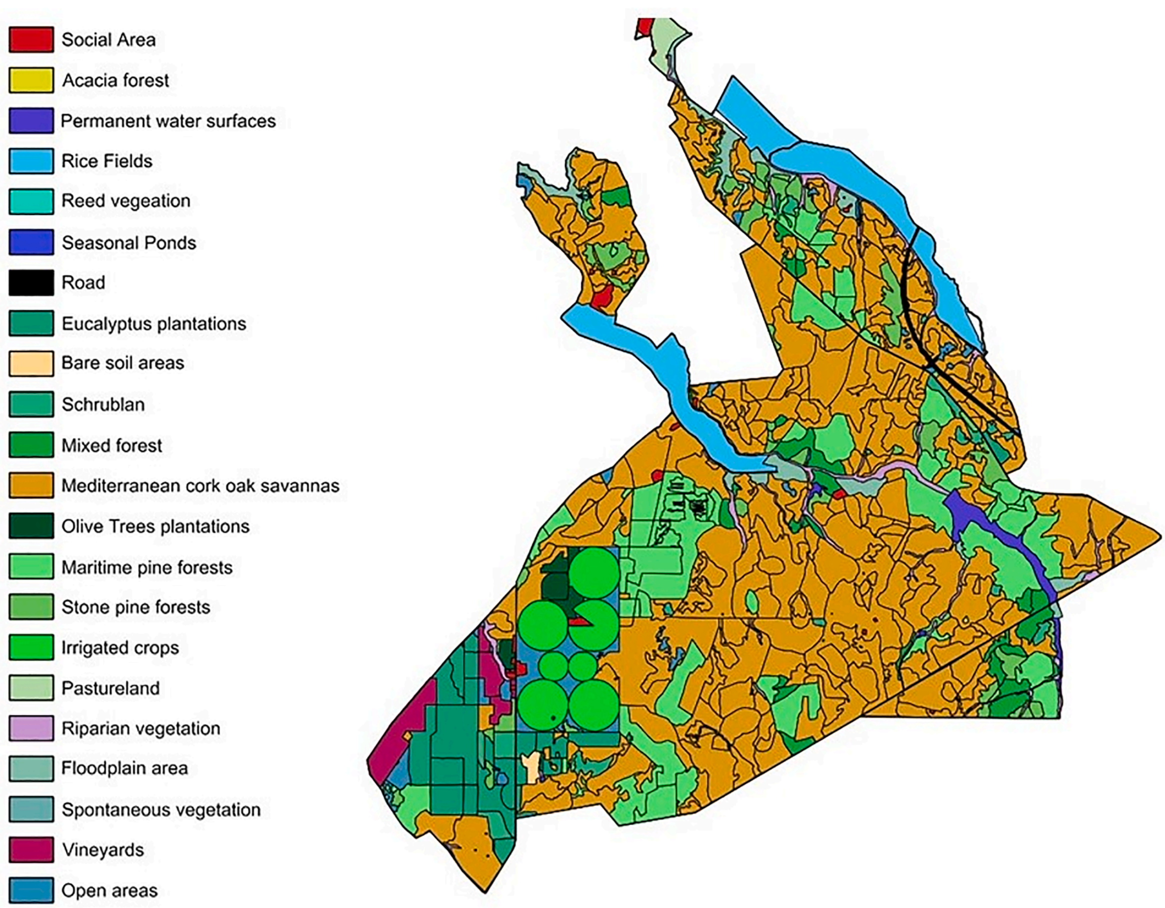

Fig. 7. 2018 LCLU map of "Charneca do Infantado"proposed by Fernandes et al. (2019) using 22 LCLU categories.

sensor (e.g., Sentinel-2, Worldview) or even by adopting a multi-sensor approach (e.g., Worldview + Sentinel-2), especially in geographical regions with frequent cloud-cover (e.g., mountainous, insular or tropical areas) and chronic scarcity of suitable and workable multispectral data. Finally, the option of developing and testing a third approach consisting of combining both RaoC and RaoMD outputs ("classic + multidimensional") to get a unique binary map representing the detected LCLU changes in the study area, has slightly improved the overall accuracy results (0.92) regarding the two initial options.

The "Example of a policy-support application" that we present in 4.2 illustrates the potential and pertinence of implementing the *spectralrao-monitoring* workflow to minimize unnecessary and expensive on-site LCLU-related control actions in multifunctional agricultural areas. It could allow regional/national controlling agencies to focus their limited

Table 4
Quantification for each LCLU/vegetation category (in hectares) shows the total area and the respective subareas identified as P0, P1 or P2 priority level for on-site controlling, according to their type of changes.

LCLU category	*P0* (in ha)	*P1* (in ha)	*P2* (in ha)
Social Area	*60.28*	*1.96*	~ 0
Acacia forest	*0.97*	~ 0	~ 0
Permanent water surfaces	*89.40*	*2.46*	*4.35*
Rice Fields	*469.75*	*193.17*	*1.98*
Reed vegetation	*4.07*	*0.11*	*0.04*
Seasonal Ponds	*7.13*	*0.55*	~ 0
Road	*60.88*	*0.05*	~ 0
Eucalyptus plantations	*525.86*	*38.56*	*7.46*
Bare soil areas	*15.49*	*0.36*	*1.12*
Schrubland	*132.48*	*3.34*	*0.44*
Mixed forest	*277.81*	*0.32*	*1.09*
Mediterranean cork oak savannas	*6402.01*	*320.19*	*5.09*
Olive Trees plantations	*74.82*	~ 0	*0.16*
Maritime pine forests	*1492.45*	*0.89*	*1.10*
Stone pine forests	*386.04*	*1.23*	*0.77*
Irrigated crops	*187.44*	*235,19*	*18.37*
Pastureland	*30.53*	*11.29*	*2.66*
Riparian vegetation	*201.24*	*0.92*	*0.69*
Floodplain area	*170.94*	*37.77*	*6.59*
Spontaneous vegetation	*5.31*	*~ 0*	*~ 0*
Vineyards	*145.09*	*3.42*	*3.89*
Open areas	*196.53*	*22.37*	*4.74*

resources on the areas where relevant LCLU/vegetation changes were effectively detected.

This study was conducted using desktop/laptop-based limited computational resources, which is still common for most remote sensing and digital agriculture scientists/practitioners, especially in public institutions. By comparing the results obtained through RaoQ-based methodological approaches with different data requirements (e.g., RaoC, RaoMD, "classic + multidimensional"), and by concluding that they are pretty close in terms of overall accuracy, we were also able to guide users towards the most suitable solution for each case.

The *spectralrao-monitoring* application can be easily accessed and reproduced thanks to a Python repository available at https://github.com/AndreaTassi23/spectralrao-monitoring. As a dynamic, high-level, free, and open-source programming language, Python can support object-oriented programming and procedural-oriented programming. It can also be easily integrated with other languages (e.g., C, C++). Python supports several relevant geospatial libraries to perform various basic and advanced geoprocessing and image processing analytical tasks (e.g., GDAL, LibLAS), providing complete interoperability with GIS and remote sensing-based platforms and frameworks. In terms of computational resources, the execution of the *spectralrao-monitoring* workflow may be demanding. Its application in vast study areas or its use with high/very-high spatial resolution data might require more powerful hardware or the use of a cloud-based platform. This is particularly true

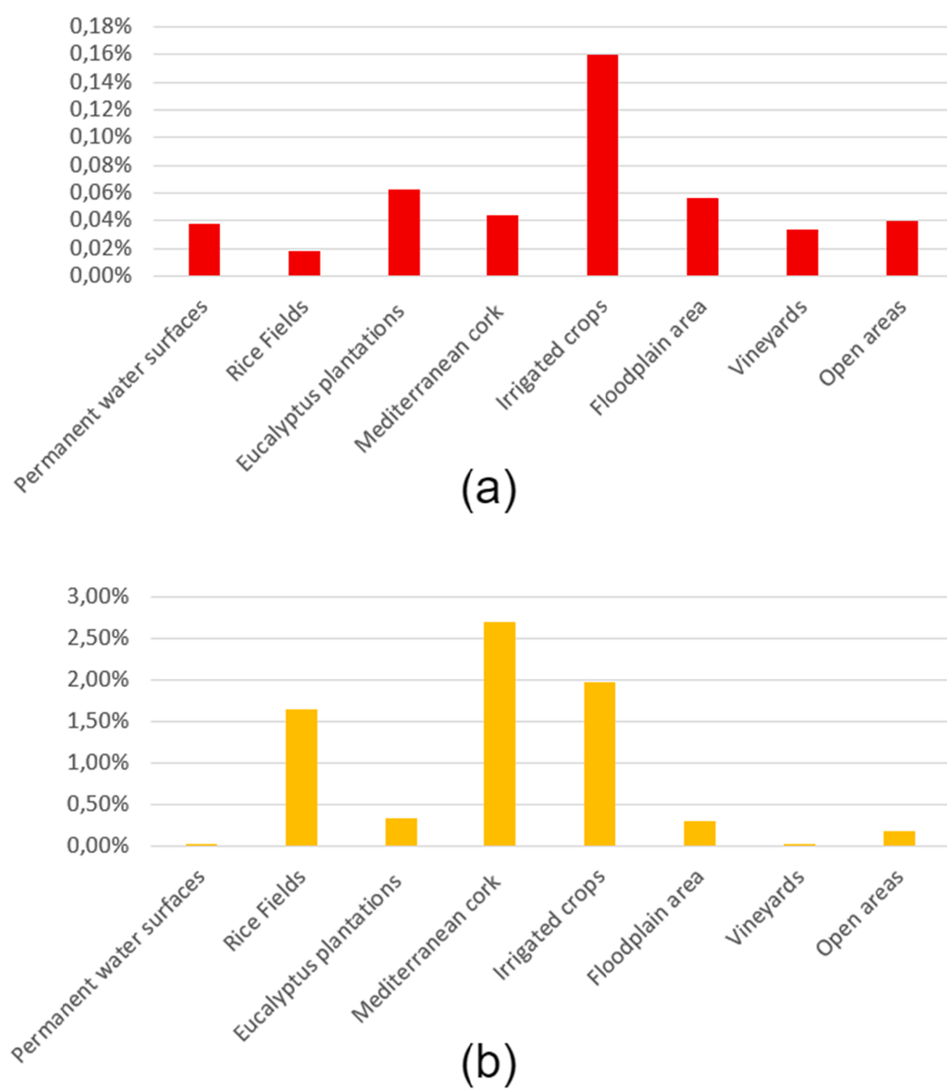

Fig. 8. Relation (in percentage) between LCLU/vegetation categories and their on-site controlling priority-level assessment: P1 (a) and P2 (b).

for the calculation of RaoC and RaoMD, as the use of the moving window centered for each pixel allows the extraction of textural information, and the resulting performance might be relatively slow, especially for larger study areas and higher spatial resolutions. The other workflow steps are swift and require low computational resources since all the georeferenced images are converted into NumPy, and the classification processes are based on an automatic threshold. Authors encourage the open-source development and implementation of this application in geospatial cloud-based computing platforms, especially Google Earth Engine, because of its global popularity and active users' community.

Based on this case study, we can conclude that this RaoQ-based application may constitute a straightforward and reliable LCLU change monitoring tool for multifunctional agricultural areas. It can be used as a low-cost decision-support tool to quickly and effectively increase the cost-benefit ratio of the on-site LCLU-related controlling actions, namely those related to the monitoring of subsidized areas for agricultural production or agri-environmental schemes implementation.

Declaration of Competing Interest

The authors declare that they have no known competing financial interests or personal relationships that could have appeared to influence the work reported in this paper.

Acknowledgments

The authors dedicate this work to the memory of Mr. Franco Tassi.

Authors gratefully acknowledge Professor Duccio Rocchini (Alma Mater Studiorum University of Bologna, Italy) for developing and freely providing in his GitHub repository (https://github.com/mattmar/spectralrao) the Rao's Q diversity index's R script.

Authors gratefully acknowledge the authors led by Fernandes et al. (2019) for providing us the 2018 LCLU/vegetation map of "Charneca do Infantado" in GIS format.

Author A.Tassi gratefully acknowledges the Erasmus + Mobility Programme to allow his traineeship at the University of the Azores from May to September 2019.

During the conception and primary development of this research idea, author A. Gil was funded by FCT (Portuguese National Foundation for Science and Technology) under a postdoctoral fellowship (SFRH/BPD/100017/2014) and a subsequent Assistant Researcher contract (Decree-Law 57/2017).

References

Abdulkareem, J.H., Sulaiman, W.N.A., Pradhan, B., Jamil, N.R., 2018. Relationship between design floods and land use land cover (LULC) changes in a tropical complex catchment. Arab. J. Geosci. 11 (14) https://doi.org/10.1007/s12517-018-3702-4.

Aboelnour, M., Engel, B.A., 2018. Application of Remote Sensing Techniques and Geographic Information Systems to Analyze Land Surface Temperature in Response to Land Use/Land Cover Change in Greater Cairo Region. JGIS 10 (01), 57–88. https://doi.org/10.4236/jgis.2018.101003.

Balamurugan, G., Aravind, S.M., 2015. Land use land cover changes in pre- and postearthquake affected area using geoinformatics - Western Coast of Gujarat, India. Disaster Adv.

Botta-Dukát, Z., 2005. Rao's quadratic entropy as a measure of functional diversity based on multiple traits. J. Veg. Sci. https://doi.org/10.1658/1100-9233(2005)16[533:rqeaam]2.0.co;2.

Cairol, D., Coudel, E., Knickel, K., Caron, P., Kröger, M., 2009. Multifunctionality of agriculture and rural areas as reflected in policies: The importance and relevance of the territorial view. J. Environ. Policy Plan. 11 (4), 269–289. https://doi.org/10.1080/15239080903033846.

Casini, L., Contini, C., Romano, C., 2012. Paths to developing multifunctional agriculture: Insights for rural development policies. Int. J. Agric. Resour. Gov. Ecol. 9 (3/4), 185. https://doi.org/10.1504/IJARGE.2012.050347.

Chaves, M.E.D., Picoli, M.C.A., Sanches, I.D., 2020. Recent applications of Landsat 8/OLI and Sentinel-2/MSI for land use and land cover mapping: A systematic review. Remote Sens. https://doi.org/10.3390/rs12183062.

Chavez, P.S., 1996. Image-based atmospheric corrections - Revisited and improved. Photogramm. Eng. Remote Sensing.

Congedo, L., 2019. Semi-Automatic Classification Plugin Documentation Release 6.2.0.1. Release.

Coppin, P., Jonckheere, I., Nackaerts, K., Muys, B., Lambin, E., 2004. Digital change detection methods in ecosystem monitoring: A review. Int. J. Remote Sens. https://doi.org/10.1080/0143116031000101675.

Costa, M.H., Botta, A., Cardille, J.A., 2003. Effects of large-scale changes in land cover on the discharge of the Tocantins River. J. Hydrology 283 (1-4), 206–217. https://doi.org/10.1016/S0022-1694(03)00267-1.

European Commission: "Agri-environmental indicators" – Last access on 11 January 2022: http://ec.europa.eu/eurostat/statistics-explained/index.php/Agri-environmental_indicators.

European Commission (2006) COM/2006/0508 final: Communication from the Commission to the Council and the European Parliament - Development of agri-environmental indicators for monitoring the integration of environmental concerns into the Common Agricultural Policy. Available online at https://nam11.safelinks.protection.outlook.com/?url=https%3A%2F%2Feur-lex.europa.eu%2Flegal-content%2FEN%2FALL%2F%3Furi%3DCELEX%3A52006DC0508&data=04%7C01%7Cn.tallassery%40elsevier.com%7C2ab04982c0ff478d65c708da0b85905b%7C9274ee3f94254109a27f9fb15c10675d%7C0%7C0%7C637834965530921568%7CUnknown%7CTWFpbGZsb3d8eyJWIjoiMC4wLjAwMDAiLCJQIjoiV2luMzIiLCJBTiI6Ik1haWwiLCJXVCI6Mn0%3D%7C3000&sdata=e8j9S48iCQgbkXxTCVP%2F4%2Fy7gI5pnG9JalrqdhxljbM%3D&reserved=0.

Fernandes, J., Petrucci-Fonseca, F., Santos-Reis, M., Rosalino, L.M., 2019. Drivers of Psammodromus algirus abundance in a Mediterranean agroforestry landscape. Agrofor. Syst. 93 (6), 2281–2291. https://doi.org/10.1007/s10457-019-00348-w.

Gil, A., Fonseca, C., Benedicto-Royuela, J., 2018. Land Cover Trade-offs in Small Oceanic Islands: A Temporal Analysis of Pico Island. Land Degrad Dev 29 (2), 349–360. https://doi.org/10.1002/ldr.2770.

Gorelick, N., Hancher, M., Dixon, M., Ilyushchenko, S., Thau, D., Moore, R., 2017. Remote Sensing of Environment Google Earth Engine : Planetary-scale geospatial analysis for everyone. Remote Sens. Environ. https://doi.org/10.1016/j.rse.2017.06.031.

Gullino, P., Battisti, L., Larcher, F., 2018. Linking multifunctionality and sustainability for valuing peri-urban farming: A case study in the Turin Metropolitan Area (Italy). Sustain 10 (5), 1625. https://doi.org/10.3390/su10051625.

Hansen, M.C., Potapov, P.V., Moore, R., Hancher, M., Turubanova, S.A., Tyukavina, A., Thau, D., Stehman, S.V., Goetz, S.J., Loveland, T.R., Kommareddy, A., Egorov, A., Chini, L., Justice, C.O., Townshend, J.R.G., 2013. High-Resolution Global Maps of 21st-Century Forest Cover Change. Science 342 (6160), 850–853.

Hansen, M.C., Egorov, A., Potapov, P.V., Stehman, S.V., Tyukavina, A., Turubanova, S.A., Roy, D.P., Goetz, S.J., Loveland, T.R., Ju, J., Kommareddy, A., Kovalskyy, V., Forsyth, C., Bents, T., 2014. Monitoring conterminous United States (CONUS) land cover change with Web-Enabled Landsat Data (WELD). Remote Sens. Environ. 140, 466–484. https://doi.org/10.1016/j.rse.2013.08.014.

Https://www.usgs.gov/core-science-systems/nli/landsat/landsat-level-1-processing-details, n.d. Terrain Precision Correction processing level (L1TP) [WWW Document].

Huylenbroeck, G. Van, Durand, G., 2003. Multifunctionality and rural development: a general framework, in: Multifunctional Agriculture: A New Paradigm for European Agriculture and Rural Development.

Khare, S., Latifi, H., Rossi, S., 2021. A 15-year spatio-temporal analysis of plant β-diversity using Landsat time series derived Rao's Q index. Ecol. Indic. 121, 107105. https://doi.org/10.1016/j.ecolind.2020.107105.

Lillesand, T.M., Kiefer, R.W., 2000. Remote sensing and image interpretation. John Wiley and Sons. New York, USA. p736.

Lobell, D.B., Thau, D., Seifert, C., Engle, E., Little, B., 2015. A scalable satellite-based crop yield mapper. Remote Sens. Environ. 164, 324–333. https://doi.org/10.1016/j.rse.2015.04.021.

Lomba, A., Guerra, C., Alonso, J., Honrado, J.P., Jongman, R., McCracken, D., 2014. Mapping and monitoring High Nature Value farmlands: Challenges in European landscapes. J. Environ. Manage. 143, 140–150. https://doi.org/10.1016/j.jenvman.2014.04.029.

Lunetta, R.S., Knight, J.F., Ediriwickrema, J., Lyon, J.G., Worthy, L.D., 2006. Land-cover change detection using multi-temporal MODIS NDVI data. Remote Sens. Environ. 105 (2), 142–154. https://doi.org/10.1016/j.rse.2006.06.018.

Madonsela, S., Cho, M.A., Ramoelo, A., Mutanga, O., 2021. Investigating the Relationship between Tree Species Diversity and Landsat-8 Spectral Heterogeneity across Multiple Phenological Stages. Remote Sens. 13, 2467. https://doi.org/10.3390/rs13132467.

Oliver, T.H., Heard, M.S., Isaac, N.J.B., Roy, D.B., Procter, D., Eigenbrod, F., Freckleton, R., Hector, A., Orme, C.D.L., Petchey, O.L., Proença, V., Raffaelli, D., Suttle, K.B., Mace, G.M., Martín-López, B., Woodcock, B.A., Bullock, J.M., 2015. Biodiversity and Resilience of Ecosystem Functions. Trends Ecol. Evol. 30 (11), 673–684. https://doi.org/10.1016/j.tree.2015.08.009.

Palmer, M.W., Earls, P.G., Hoagland, B.W., White, P.S., Wohlgemuth, T., 2002. Quantitative tools for perfecting species lists. Environmetrics 13 (2), 121–137.

Podani, J., 2000. Distance, similarity, correlation. Introd. to Explor. Multivar. Biol. Data.

Ramankutty, N., Foley, J.A., 1999. Estimating historical changes in global land cover: Croplands from 1700 to 1992. Global Biogeochem. Cycles. 13 (4), 997–1027. https://doi.org/10.1029/1999GB900046.

Ramos-Bernal, R., Vázquez-Jiménez, R., Romero-Calcerrada, R., Arrogante-Funes, P., Novillo, C., 2018. Evaluation of unsupervised change detection methods applied to landslide inventory mapping using ASTER imagery. Remote Sens 10 (12), 1987. https://doi.org/10.3390/rs10121987.

Rao, C.R., 1982. Diversity and dissimilarity coefficients: A unified approach. Theor. Popul. Biol. 21 (1), 24–43. https://doi.org/10.1016/0040-5809(82)90004-1.

Rocchini, D., Balkenhol, N., Carter, G.A., Foody, G.M., Gillespie, T.W., He, K.S., Kark, S., Levin, N., Lucas, K., Luoto, M., Nagendra, H., Oldeland, J., Ricotta, C., Southworth, J., Neteler, M., 2010. Remotely sensed spectral heterogeneity as a proxy of species diversity: Recent advances and open challenges. Ecological Informatics 5 (5), 318–329. https://doi.org/10.1016/j.ecoinf.2010.06.001.

Rocchini, D., Chiarucci, A., Loiselle, S.A., 2004. Testing the spectral variation hypothesis by using satellite multispectral images. Acta Oecologica 26 (2), 117–120. https://doi.org/10.1016/j.actao.2004.03.008.

Rocchini, D., Marcantonio, M., Ricotta, C., 2017. Measuring Rao's Q diversity index from remote sensing: An open source solution. Ecol. Indic. 72, 234–238. https://doi.org/10.1016/j.ecolind.2016.07.039.

Rocchini, D., Thouverai, E., Marcantonio, M., Iannacito, M., Da Re, D., Torresani, M., Bacaro, G., Bazzichetto, M., Bernardi, A., Foody, G.M., Furrer, R., Kleijn, D., Larsen, S., Lenoir, J., Malavasi, M., Marchetto, E., Messori, F., Montaghi, A., Moudrý, V., Naimi, B., Ricotta, C., Rossini, M., Santi, F., Santos, M.J., Schaepman, M. E., Schneider, F.D., Schuh, L., Silvestri, S., Ŝímová, P., Skidmore, A.K., Tattoni, C., Tordoni, E., Vicario, S., Zannini, P., Wegmann, M., 2021. rasterdiv—An Information Theory tailored R package for measuring ecosystem heterogeneity from space: To the origin and back. Methods Ecol Evol 12 (6), 1093–1102.

Rouse, J.W., Haas, R.H., Schell, J.A., Deering, D.W., 1974. Monitoring vegetation systems in the great plains with ERTS. Proceedings of the Third ERTS-1 Symposium. NASA, Washington, D.C., pp. 309–317

Sachs, J., Remans, R., Smukler, S., Winowiecki, L., Andelman, S.J., Cassman, K.G., Castle, D., DeFries, R., Denning, G., Fanzo, J., Jackson, L.E., Leemans, R., Lehmann, J., Milder, J.C., Naeem, S., Nziguheba, G., Palm, C.A., Pingali, P.L., Reganold, J.P., Richter, D.D., Scherr, S.J., Sircely, J., Sullivan, C., Tomich, T.P., Sanchez, P.A., 2010. Monitoring the world's agriculture. Nature 466 (7306), 558–560. https://doi.org/10.1038/466558a.

Schmidtlein, S., Fassnacht, F.E., 2017. The spectral heterogeneity hypothesis does not hold across landscapes. Remote Sens. Environ. 192, 114–125.

Shao, P., Shi, W., He, P., Hao, M., Zhang, X., 2016. Novel Approach to Unsupervised Change Detection Based on a Robust Semi-Supervised FCM Clustering Algorithm. Remote Sens 8 (3), 264. https://doi.org/10.3390/rs8030264.

Slámová, M., Belčáková, I., 2019. The role of small farm activities for the sustainable management of agricultural landscapes: Case studies from Europe. Sustain 11 (21), 5966. https://doi.org/10.3390/su11215966.

Tassi, A., Gigante, D., Modica, G., Di Martino, L., Vizzari, M., 2021. Pixel-vs. Object-based landsat 8 data classification in google earth engine using random forest: The case study of maiella national park. Remote Sens. 10.3390/rs13122299.

Tassi, A., Gil, A., 2020. A Low-cost Sentinel-2 Data and Rao's Q Diversity Index-based Application for Detecting, Assessing and Monitoring Coastal Land-cover/Land-use Changes at High Spatial Resolution. J. Coast. Res. 10.2112/SI95-253.1.

Tassi, A., Vizzari, M., 2020. Object-Oriented LULC Classification in Google Earth Engine Combining SNIC, GLCM, and Machine Learning Algorithms. Remote Sens.

Thunig, H., Wolf, N., Naumann, S., Siegmund, A., Jürgens, C., Uysal, C., Maktav, D., 2011. Land use/land cover classification for applied urban planning - The challenge of automation, in: 2011 Joint Urban Remote Sensing Event, JURSE 2011 - Proceedings. 10.1109/JURSE.2011.5764762.

Torresani, M., Feilhauer, H., Rocchini, D., Féret, J.-B., Zebisch, M., Tonon, G., 2021. Which optical traits enable an estimation of tree species diversity based on the Spectral Variation Hypothesis? Appl. Veg. Sci. 24 (2) https://doi.org/10.1111/avsc.v24.210.1111/avsc.12586.

Torresani, M., Rocchini, D., Sonnenschein, R., Zebisch, M., Marcantonio, M., Ricotta, C., Tonon, G., 2019. Estimating tree species diversity from space in an alpine conifer forest: The Rao's Q diversity index meets the spectral variation hypothesis. Ecological Informatics 52, 26–34. https://doi.org/10.1016/j.ecoinf.2019.04.001.

Vázquez-Jiménez, R., Ramos-Bernal, R.N., Romero-Calcerrada, R., Arrogante-Funes, P., Tizapa, S.S., Novillo, C.J., 2018. Thresholding Algorithm Optimization for Change Detection to Satellite Imagery, in: Colorimetry and Image Processing. 10.5772/intechopen.71002.

Williams, H., Colombi, T., Keller, T., 2020. The influence of soil management on soil health: An on-farm study in southern Sweden. Geoderma 360, 114010. https://doi.org/10.1016/j.geoderma.2019.114010.

Wilson, G.A., 2009. The spatiality of multifunctional agriculture: A human geography perspective. Geoforum 40 (2), 269–280. https://doi.org/10.1016/j.geoforum.2008.12.007.

Woodcock, C.E., Macomber, S.A., Kumar, L., 2010. Vegetation mapping and monitoring, in: Environmental Modelling with GIS and Remote Sensing. 10.4324/9780203302217_chapter_6.

Zhang, T., Su, J., Liu, C., Chen, W.H., Liu, H., Liu, G., 2017. Band selection in sentinel-2 satellite for agriculture applications, in: ICAC 2017 - 2017 23rd IEEE International Conference on Automation and Computing: Addressing Global Challenges through Automation and Computing. 10.23919/IConAC.2017.8081990.